Available online at www.sciencedirect.com
ScienceDirect
Journal of Power Sources 163 (2006) 500–508
JOURNAL OF POWER SOURCES
www.elsevier.com/locate/jpowsour

An investigation into polypyrrole-coated 316L stainless steel as a bipolar plate material for PEM fuel cells

Yan Wang, Derek O. Northwood *

Department of Mechanical, Automotive, and Materials Engineering, University of Windsor, 401 Sunset Avenue, Windsor, Ontario, Canada N9B 3P4

Received 17 August 2006; received in revised form 20 September 2006; accepted 20 September 2006
Available online 7 November 2006

Abstract

Increasing attention is being paid to the use of metallic materials as a replacement for non-porous graphite in bipolar plates (BPs) for polymer exchange membrane (PEM) fuel cells. The ideal BP material should demonstrate high values of electrical conductivity, thermal conductivity, corrosion resistance and compressive strength and low values of gas permeability and density. Although metallic materials demonstrate many of those properties, their corrosion resistance can be inadequate, which in turn can lead to unacceptable values of contact resistivity. In this study, polypyrrole was polymerized onto 316L stainless steel using galvanostatic and cyclic voltammometric methods. A dense coating of polypyrrole could be formed on SS316L using both electrochemical methods. The coatings had different morphologies. For galvanostatic coatings, the particle size increases with increasing applied current. For cyclic voltammometric coatings, the particle size increases with increasing the cycle number. The potentiodynamic tests show that the corrosion current density is decreased by about one order of magnitude and polarization resistance is increased by about one order of magnitude by coating with polypyrrole. Optical microscopy showed that there is less intergranular corrosion after coating with polypyrrole. Therefore, these dense polypyrrole coatings much improved the corrosion resistance of SS316L and the coated materials could possibly be used in polymer exchange membrane fuel cells (PEMFCs) as a bipolar plate material.

Keywords: Bipolar plates; Polypyrrole; Galvanostatic; Cyclic voltammometric; Corrosion

1. Introduction

With escalating oil prices and increasing environmental concerns, increasing attention is being paid to the development of fuel cells. Polymer exchange membrane fuel cells (PEMFCs) are one of the most important fuel cells and have been extensively researched because PEMFCs operate at low temperatures and allow rapid start-up. The present cost of PEMFCs is about US$ 200 kW^{-1} which is a major barrier for commercialization in automotive applications [1]. Bipolar plates are one of the most important components in PEM fuel cells. They are designed to accomplish many functions, including: distribute the fuel and oxidant in the stack, facilitate water management within the cell, separate the individual cells in the stack, carry current away from the cell, and facilitate heat management. Efforts are underway to develop bipolar plates that satisfy these demands. Currently, the main commercial bipolar plates are made of non-porous graphite because graphite is chemically and thermally stable in a fuel cell environment. These non-porous graphite bipolar plates account for about 80% of the total weight and 45% of the stack cost [2]. In order to compete with an internal combustion engine, the cost of the total fuel cell stack must be reduced to US$ 50 kW^{-1} and the cost of bipolar plates must be reduced to US$ 10 kW^{-1} [1]. However, in a PEM fuel cell stack, the cost of bipolar plates is about US$ 90 kW^{-1} which is far too expensive [1,2]. Thus, there is increasing interest in finding less expensive materials from which to manufacture bipolar plates for PEM fuel cells.

Metals have good mechanical stability, electrical conductivity and thermal conductivity and can be recyclable. Furthermore, they can be easily stamped to a desired shape to accommodate the flow channels in the fuel cell. In a PEMFC environment, metals are prone to corrosion and the resulting metal ions can readily migrate to, and poison, the membrane. The dissolved metal ions lower the ionic conductivity of the membrane and, thus, the performance of the PEMFC. Furthermore, any corrosion layer will lower the electrical conductivity of the bipolar plates, and

* Corresponding author. Tel.: +1 519 253 3000x4785; fax: +1 519 973 7007.
E-mail address: dnorthwo@uwindsor.ca (D.O. Northwood).

0378-7753/$ – see front matter © 2006 Elsevier B.V. All rights reserved.
doi:10.1016/j.jpowsour.2006.09.048

increase the potential loss because of a higher electrical resistance. Hence, in order to be suitable materials of bipolar plates, metals should have both a very high corrosion resistance and electrical conductivity. Several metals including stainless steel, aluminum, titanium, and nickel are being researched world-wide [3].

Conductive polymers are a new type of material which has a high redox potential and properties of both metals and plastics. Electrochemical polymerization of conductive polymers has received wide attention because of its simplicity and the fact that it is a one-step process [4]. Polymers have been deposited on aluminium and stainless steel to improve the corrosion resistance of these metals [5–9]. Polypyrrole is one of the most researched conductive polymers that have been deposited on metal surfaces. Joseph et al. [8] have reported that polypyrrole and polyaniline coatings, deposited using a cyclic voltammometric method, can provide corrosion protection for metallic bipolar plates. In their paper, they concluded that the polymer-coated 304 stainless steel plates showed improved corrosion resistance with an acceptable contact resistance. The corrosion tests were, however, evaluated in a 0.1 M H_2SO_4 solution and not in actual PEMFC working condition. In this study, polypyrrole was deposited on the surface of 316L stainless steel using both galvanostatic and cyclic voltammometric methods. Optical microscopy, SEM, and electrochemical tests were used to characterize the coated samples. Some preliminary results have already been reported [10].

2. Experimental

2.1. Base material and its polarization

SS316L was chosen as the base material primarily because of its good corrosion resistance. The chemical analysis of the SS316L used in this study is given in Table 1. The plates were cut into samples 1.5 cm × 1.5 cm (area = 2.25 cm^2). An electrical contact was made to one side by means of nickel print. Then the contact side and the edges of the metal sample were sealed with epoxy resin, leaving one side for polymerization and characterization [11]. Before coating, the metal samples were polished on 240 grit silicon carbide papers to form a coarse surface in order to increase the adhesion between the metal and the coating. In the corrosion testing of the uncoated metal, the samples were polished on 240, 600 and 800 grit silicon carbide papers and a final polish with 1.0 μm alumina powder. Potentiodynamic tests were used to measure the corrosion resistance of SS316 at both ambient (20 °C) and high (70 °C) temperatures. In the potentiodynamic tests, the initial potential was −0.1 V versus OCP, and the final potential was 1.2 V versus SCE and the scan rate was 1 mV s^{-1}. The electrolyte was a 0.5 M sulphuric acid solution.

2.2. Electropolymerization

For the coating with polypyrrole, both galvanostatic and cyclic voltammometric methods were used. In galvanostatic coating, different currents were utilized to coat polypyrrole films and the total application time was 30 min. In cyclic voltammometric coating, the initial potential was −0.2 V versus SCE and the final potential was 1.0 V versus SCE and scan rate was 5 mV s^{-1}. The number of cycles was 2, 4, 6, and 8, respectively. The electrolyte used for coating was a 0.1 M sulphuric acid and 0.1 M pyrrole solution. The electrochemical instrumentation used was a Solartron 1285 potentiostat. A typical three-electrode system was used.

2.3. Characterization

In order to observe any corrosion products and other surface changes, the samples were examined using optical microscopy [Buehler Optical Image Analyzer 2002 System]. The detailed features of the surface microstructures were also characterized at high magnifications using a JSM-5800LV scanning electron microscope (SEM).

2.4. Electrochemistry

Potentiodynamic and potentiostatic tests were utilized to analyze the corrosion characteristics of uncoated and coated metals. In order to simulate the working conditions of a PEMFC, potentiostatic tests were conducted: at the anode, the applied potential was −0.1 V versus SCE purged with H_2 and at the cathode, the applied potential was 0.6 V versus SCE purged with O_2.

3. Results

3.1. Polarization behavior of SS316 at ambient and high temperatures

As shown in Fig. 1, SS316L exhibits typical active–passive corrosion behavior. The potentiodynamic curve can be divided into three regions including an active region (−0.4 to −0.1 V), a passive region (−0.1 to 0.9 V), and a transpassive region (0.9–1.2 V). It is well known that the chromium content (16.32% in this SS316) in a stainless steel determines its corrosion resistance because chromium can form a passive film which can prevent further corrosion. Also, the nickel content (10.54% in this metal) can play an important role in the corrosion behaviour of stainless steel. Nickel has a fcc crystal structure and Ni additions enable a stainless steel to have a fcc structure at room temperature.

Comparing the two curves in Fig. 1 at the two different temperatures, the corrosion current density at the higher temperature

Table 1
Chemical composition of SS316L (wt%)

Metal	C	Mn	P	S	Si	Cr	Ni	Mo	Cu	N	Fe
SS316L	0.021	1.82	0.029	0.01	0.58	16.32	10.54	2.12	0.47	0.03	Balance

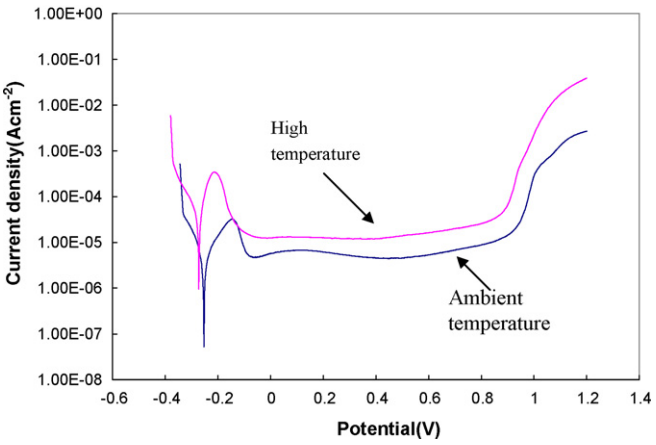

Fig. 1. Potentiodynamic curves for base SS316L at ambient (20 °C) and high (70 °C) temperatures. The electrolyte is a 0.5 M sulphuric acid solution.

is higher than that at ambient temperature. Also, the corrosion potential is slightly lower at the high temperature than that at ambient temperature. Based on the linear polarization, we can get the polarization resistance of SS316L at different temperatures.

$$R_p = \frac{\beta_a \beta_c}{2.3 i_{corr}(\beta_a + \beta_c)}, \quad (1)$$

where β_a, β_c, i_{corr}, and R_p are the Tafel slopes of the anodic and cathodic reactions, the corrosion current density, and polarization resistance, respectively [12].

From Table 2, we can see that the polarization resistance and corrosion current density at 20 °C are about 4198 Ω cm^2 and 4.891 μA cm^{-2}. However, the polarization resistance and corrosion current density at 70 °C are 340 Ω cm^2 and 40.318 μA cm^{-2}. At the elevated temperature (70 °C), the polarization resistance is thus reduced by more than one order of magnitude and the corrosion rate is increased by about one order of magnitude compared to ambient temperature. The working temperature for a PEMFC is between 60 and 100 °C. Therefore, in a PEMFC environment, the corrosion is much increased compared to corrosion at ambient temperature. According to some researchers [13,14], metal ions generated from corrosion can migrate to the membrane and levels as low as 5–10 ppm can degrade the membrane performance. Thus, in order to be suitable for use as bipolar plates, metallic materials should have a superior corrosion resistance.

3.2. Effect of roughness on polarization resistance

Because different grit silicon carbide papers were used to prepare specimens for the potentiodynamic tests and polymerization, potentiodynamic tests were conducted for different surface roughnesses in order to determine the effect of surface roughness on the polarization resistance. The results are shown in Table 3. From the results, we can see that the corrosion current density and polarization resistance are almost the same for the different surface roughness samples.

3.3. Optical microscopy

Although there is corrosion in ambient temperature potendynamic tests (based on the potentiodynamic polarization curve), we could not detect any corrosion product using optical microscopy (Fig. 2b). However, at 70 °C (Fig. 2c), we can see intergranular corrosion of the SS316L. The grain boundaries of SS316L are corroded after high temperature corrosion. Chromium carbides ($Cr_{23}C_6$) can precipitate at the grain boundaries in SS316L. When the chromium carbides form at the grain boundaries, they deplete chromium in the regions adjacent to the boundaries so that the chromium level in these areas decreases below the 12% chromium level necessary for passive behavior. These areas become anodic to the rest of the grain boundaries, which are cathodic, thus, creating galvanic couples [15]. From the corroded surface, we can see that most grains are in the 10–30 μm size range.

Table 2
Polarization parameters of SS316L at 20 and 70 °C in a 0.5 M sulphuric acid solution

Temperature (°C)	β_a (V)	β_c (V)	E_{corr} (V)	i_{corr} (μA cm^{-2})	R_p (Ω cm^2)
20	0.114	0.081	−0.251	4.891	4198
70	0.055	0.074	−0.268	40.318	340

Table 3
Polarization parameters of SS316L with different surface roughnesses at 70 °C

Polishing media	R_a (μm)	β_a (V)	β_c (V)	E_{corr} (V)	i_{corr} (μA cm^{-2})	R_p (Ω cm^2)
240 grit	–	0.052	0.072	−0.259	38.981	337
240 grit	–	0.054	0.074	−0.268	38.074	356
240 grit	–	0.057	0.075	−0.271	42.502	331
Average	0.12	–	–	−0.266	39.852	341
Alumina powder 1.0	–	0.057	0.071	−0.267	41.273	333
Alumina powder 1.0	–	0.053	0.071	−0.270	40.012	328
Alumina powder 1.0	–	0.055	0.074	−0.268	40.318	340
Average	0.05	–	–	−0.268	40.534	334

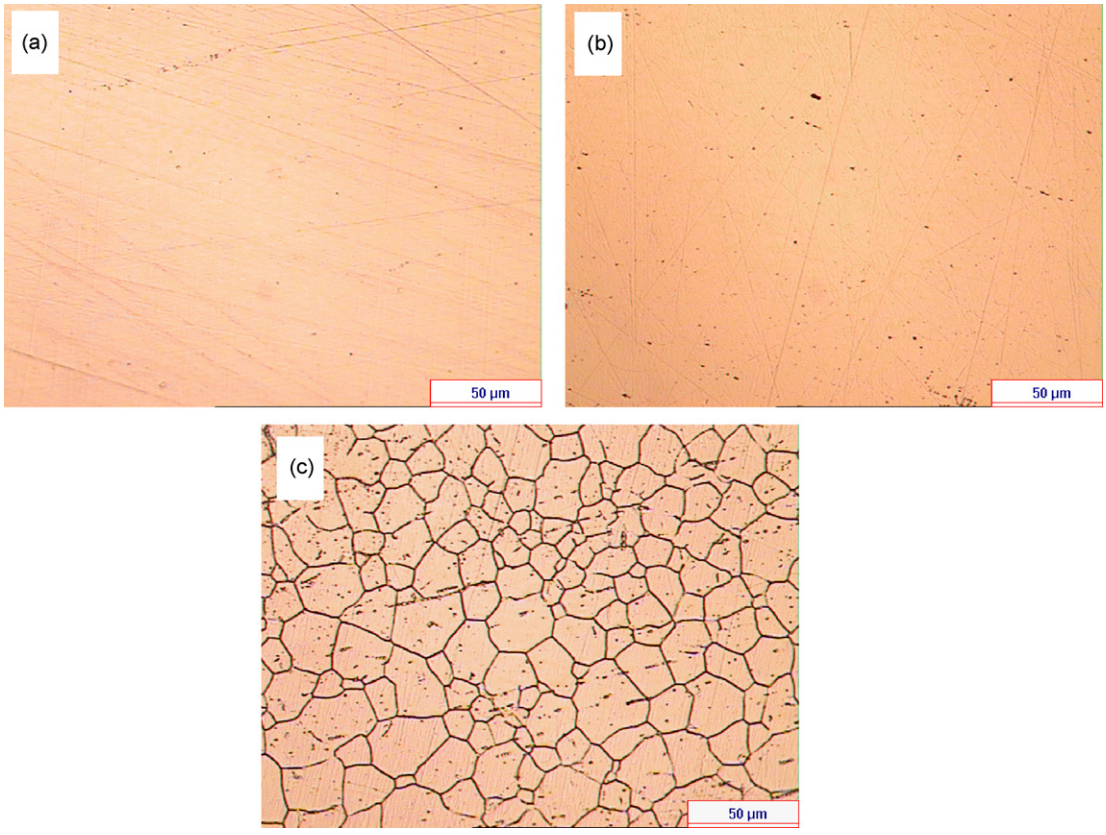

Fig. 2. Optical microscopy for SS316L: (a) before corrosion, (b) after ambient potentiodynamic testing, and (c) after high temperature potentiodynamic testing in 0.5 M sulphuric acid solution.

3.4. Electrochemical polymerization

Fig. 3 presents galvanostatic coating curves for polypyrrole on SS316L. We can see that when different currents are used to coat polypyrrole on SS316L, it gives rise to different coating potentials. When the applied current is 0.0001 A, the potential increases to about 0.36 V after a short time and then stabilizes. When the applied current is 0.0002 A, the potential is about 0.6 V after 100 s and then stabilizes. When the applied current is 0.0005 A, the potential first increases to 0.8 V and it then takes about 700 s to reach a stable potential (1.5 V). When the current is further increased to 0.001 and 0.005 A, it takes less time to reach the stable potential. However, the stable

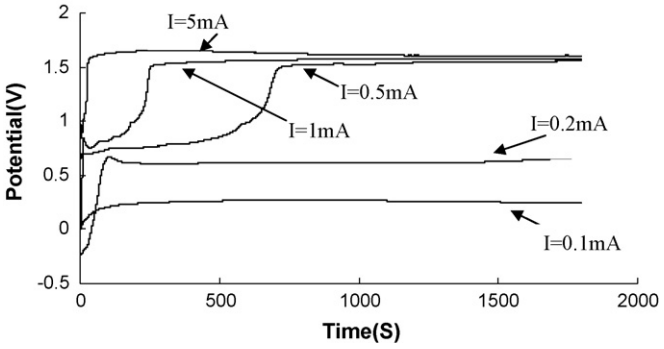

Fig. 3. Galvanostatic coating of polypyrrole on SS316L.

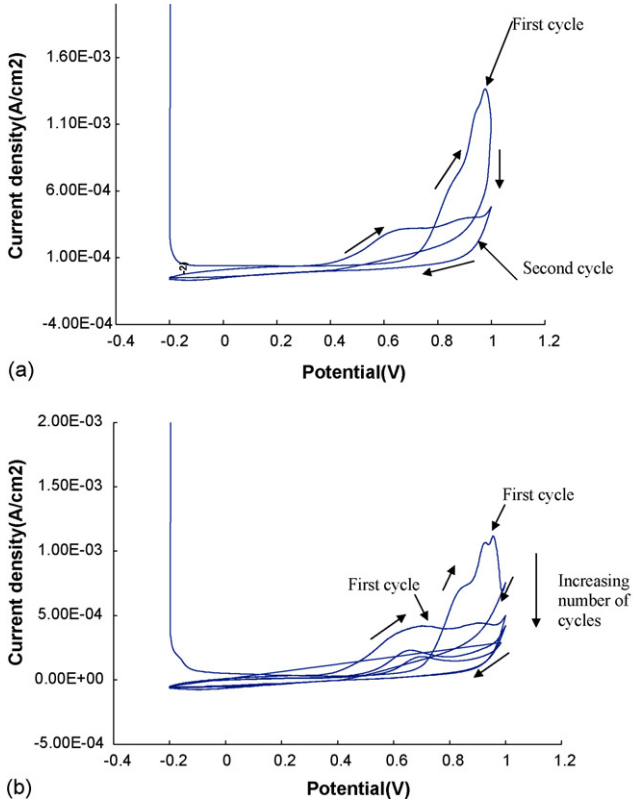

Fig. 4. Cycle voltammometric coating of polypyrrole on SS316L: (a) 2 cycles and (b) 4 cycles.

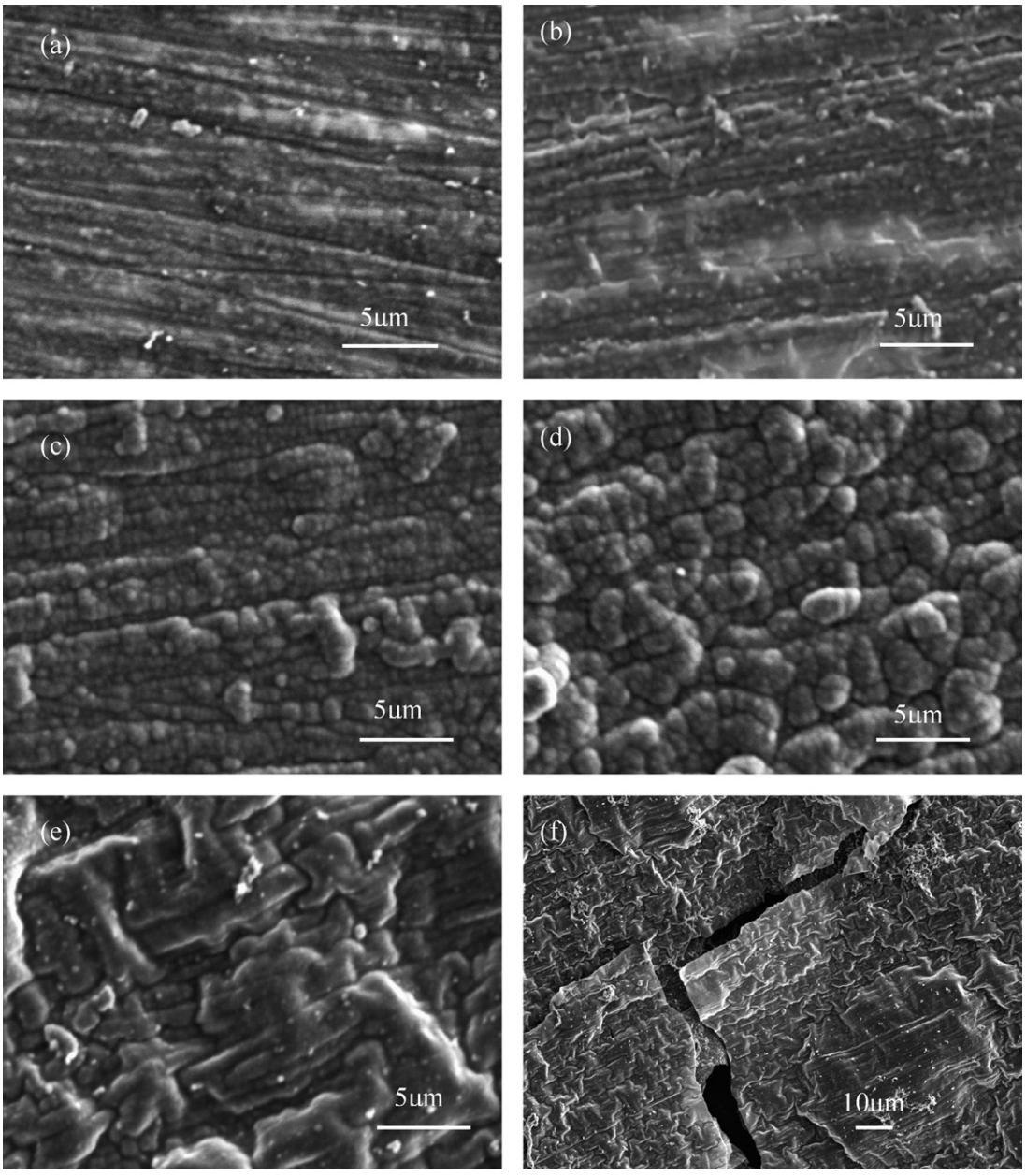

Fig. 5. SEM micrographs of SS316L coated with polypyrrole using galvanostatic method and different applied currents: (a) 0.0001 A, (b) 0.0002 A, (c) 0.0005 A, (d) 0.001 A, and (e and f) 0.005 A.

potentials are almost the same for applied currents of 0.0005, 0.001, and 0.005 A. This is because water begins to dissociate on the SS316L surface at 1.5 V versus SCE and we observed some bubbles on the metal surface.

Fig. 4 presents the cyclic voltammometric coating curves for polypyrrole on SS316L. In the first cycle, the current density is very low from −0.2 to 0.7 V. At 0.7 V, the current density begins to rapidly increase and reaches 1.0×10^{-3} A cm^{-2} at which time polypyrrole begins to form in significant amounts on the SS316L surface. In the second cycle, the maximum current density is only about 4.0×10^{-4} A cm^{-2}. Thus, there is less polypyrrole formed in the second cycle. Moreover, in the second cycle, we find that there is a wide peak at 0.7 V. From Fig. 4b, we can also see a peak at 0.7 V in the third and fourth cycles. With increasing number of cyles, the peak becomes smaller. This peak at about 0.7 V is due to the oxidation of the polypyrrole. Therefore, in the first cycle of a multi-cycle coating process, polypyrrole is formed first. In subsequent cycles, some of the polypyrrole is oxidized at about 0.7 V. The oxidation of polypyrrole helps protect the SS316L from corroding.

3.5. SEM of polypyrrole-coated materials

SEM micrographs of polypyrrole-coated SS316L produced at different applied currents and number of cycles are shown in Figs. 5 and 6. Fig. 5a and b shows the samples produced using the galvanostatic method and applied currents of 0.0001 and 0.0002 A, respectively. The polypyrrole film is quite thin

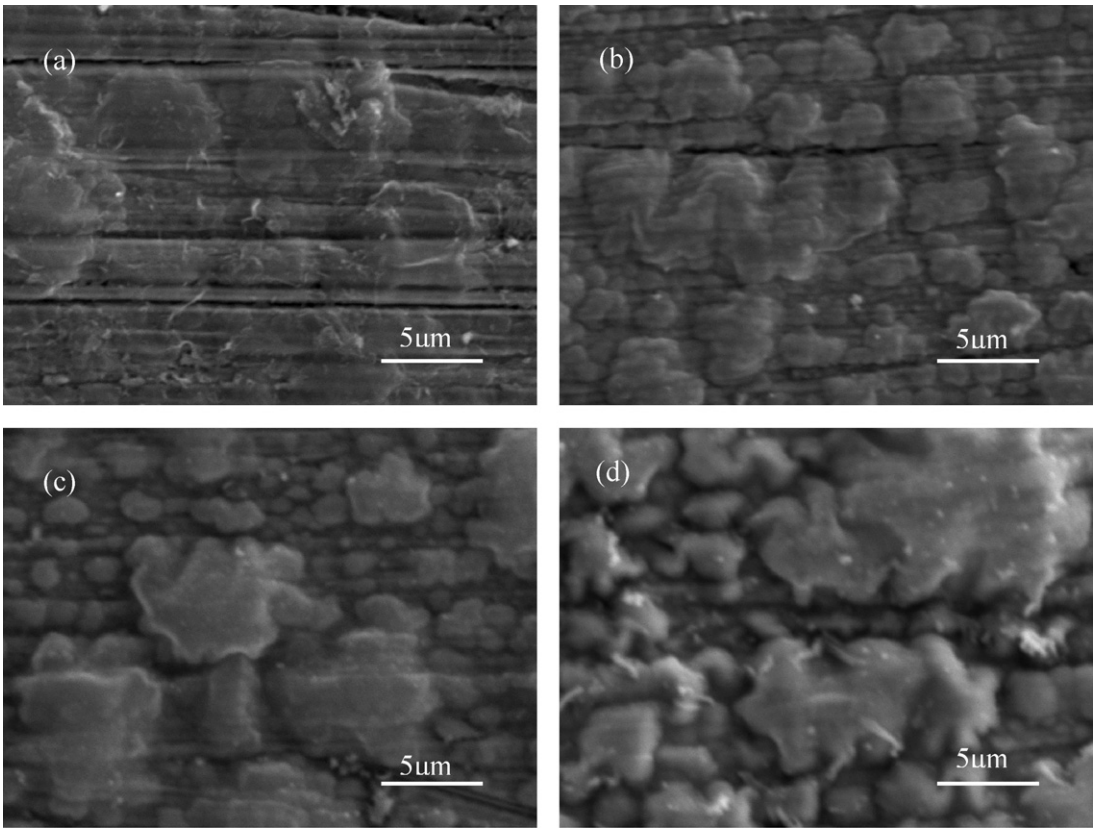

Fig. 6. SEM micrographs of SS316L coated with polypyrrole using a cyclic voltammometric method: (a) 2-cycle coating, (b) 4-cycle coating, (c) 6-cycle coating, and (d) 8-cycle coating.

and the polishing marks from the 240 grit polishing of the SS316L are still visible. When the applied current is increased to 0.0005 and 0.001 A, polypyrrole particles are seen on the SS316L surface. Most of the polypyrrole particles are smaller than 1 μm for an applied current of 0.0005 A (Fig. 5c). The polypyrrole particle size increases to 2–3 μm for an applied current of 0.001 A (Fig. 5d). When the applied current is increased to 0.005 A, the individual particle morphology can no longer be seen in the polypyrrole coating (Fig. 5e). Cracks were seen in the polypyrrole coating (Fig. 5f). The cracks are the result of gases being produced under the polypyrrole coating which generate sufficient pressure to fracture the coating. Because it is an oxidation reaction, the gas should be oxygen.

The morphology of the polypyrrole coatings produced using the cyclic voltammometric method are different from those produced using the galvanostatic method; compare Fig. 6 with Fig. 5. The polypyrrole particle size is larger for the cyclic voltammometric-produced coatings. The polypyrrole particle increases with increasing number of cycles. Again, the influence of the 240 grit polishing can be seen in the surface morphology, particularly at a lower number of cycles (similar to a lower applied current).

Table 4
Polarization resistance of uncoated and polypyrrole-coated SS316L at 70 °C

Samples	β_a (V)	β_c (V)	E_{corr} (V)	i_{corr} (μA cm^{-2})	R_p (Ω cm^2)
Uncoated	0.053	0.071	−0.270	40.012	328
Coated	0.399	−0.020	0.171	2.379	3459

3.6. Potentiodynamic polarization testing after coating with polypyrrole

In order to determine the polarization resistance after coating with polypyrrole, potentiodynamic polarization tests were conducted on the four-cycle voltammometric coated sample (Fig. 7). The polypyrrole coating results in an elevated (more positive) corrosion potential for SS316L and a lower corrosion current

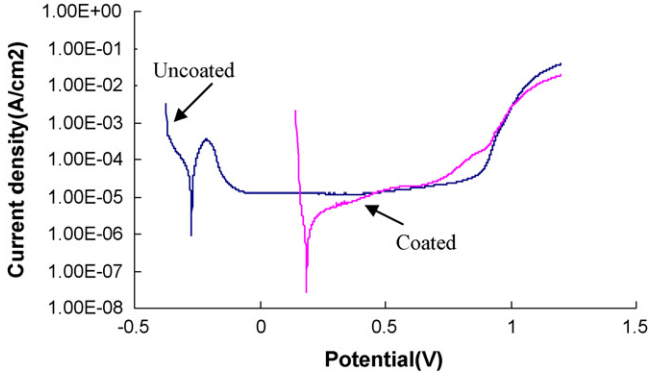

Fig. 7. Potentiodynamic polarization curve for uncoated and 4-cycle voltammometric coated SS316L at 70 °C.

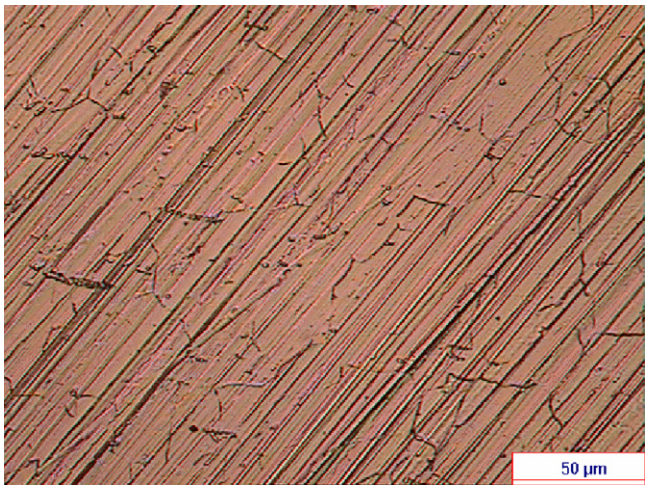

Fig. 8. Optical micrograph of 4-cycle voltammometric coated SS316L after potentiodynamic testing at 70 °C.

density from Fig. 7 and Table 4. From the linear polarization data, the polarization resistance after polypyrrole coating is more than 10 times higher than for the uncoated samples. Comparing Tables 2 and 4, we find that the polarization resistance and corrosion current density after coating at high temperature are of the same order as those of the uncoated SS316L at ambient temperature. Comparing the corrosion current densities in our work with Joseph et al. [8] results, we find that the corrosion current density ($\sim$2.4 μA cm^{-2}) in our tests is higher than that found by Joseph et al. (1 μA cm^{-2}). There are at least two possible reasons for this. First, our experiments were conducted at 70 °C, whereas Joseph et al. [8] appear to have conducted their tests at ambient temperature. The other main reason is that we used a higher concentration electrolyte for the potentiodynamic tests, 0.5 M H_2SO_4 versus 0.1 M H_2SO_4. From Fig. 7, we can also see that the current density is lower for coated SS316L below 0.6 V, but from 0.6 to 1.0 V the coated SS316L has a higher current density because polypyrrole can be oxidized, thus generating

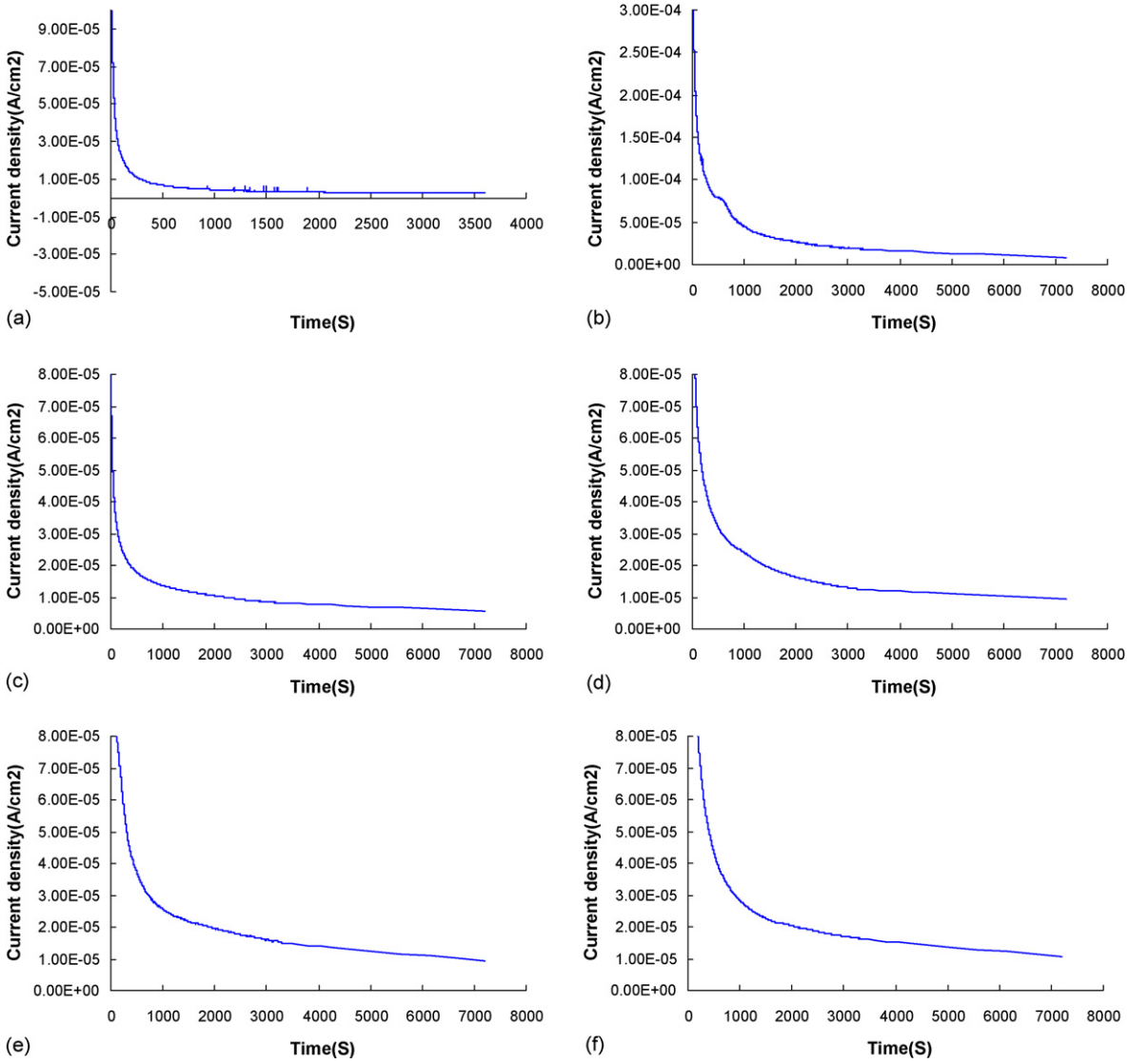

Fig. 9. Potentiostatic curves for uncoated and polypyrrole-coated SS316L at 0.6 V purged with O_2: (a) uncoated SS316L, (b) 0.0002 A coated SS316L, (c) 0.001 A coated SS316L, (d) 4-cycle coated SS316L, (e) 6-cycle coated SS316L, and (f) 8-cycle coated SS316L.

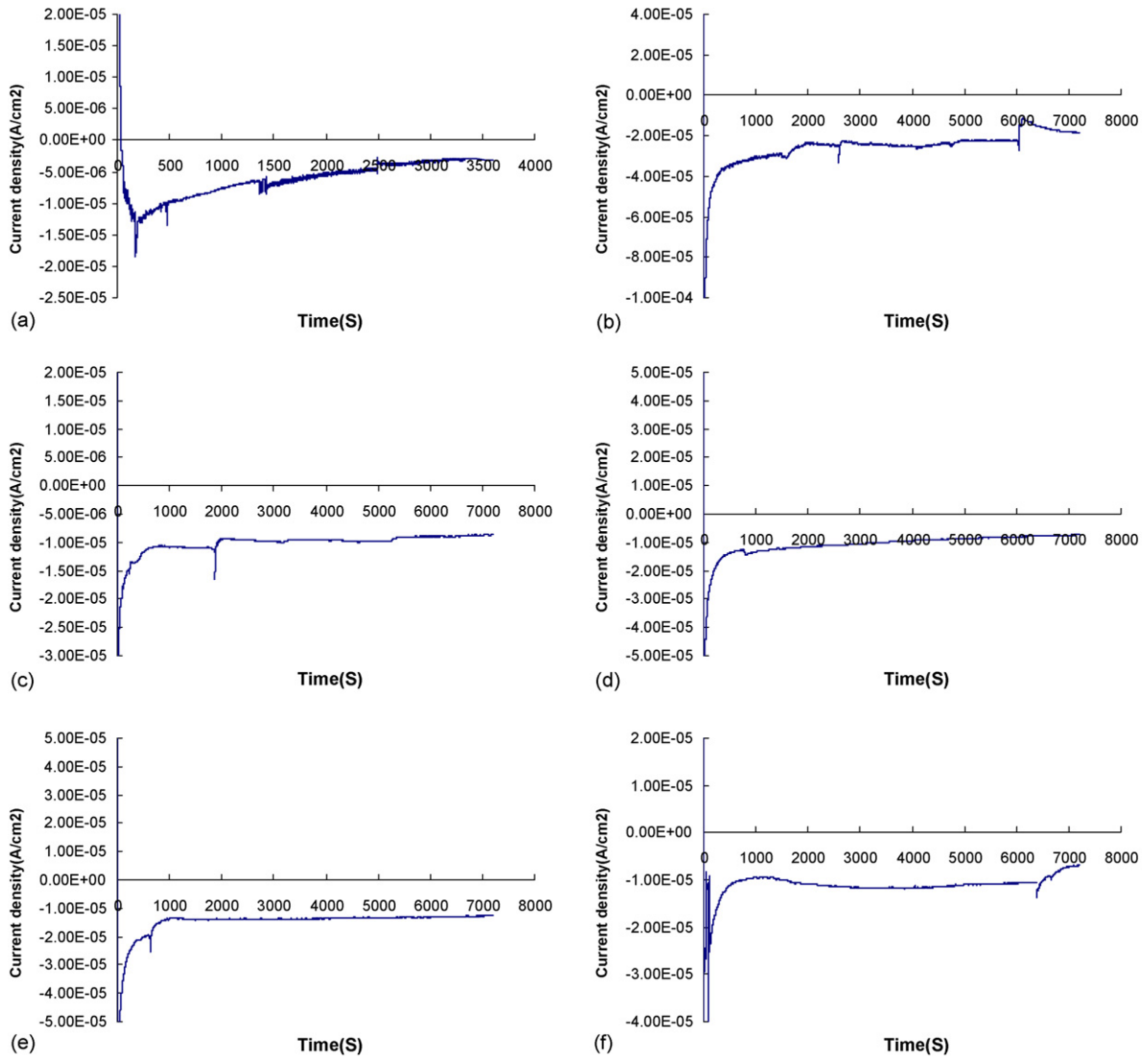

Fig. 10. Potentiostatic curves for uncoated and coated SS316 at −0.1 V purged with H_2: (a) uncoated SS316L, (b) 0.0002 A coated SS316L, (c) 0.001 A coated SS316L, (d) 4-cycle coated SS316L, (e) 6-cycle coated SS316L, and (f) 8-cycle coated SS316L.

a current. Above 1.0 V, uncoated and coated SS316L exhibit almost the same current densities.

From Fig. 8, which is an optical micrograph of a polypyrrole-coated SS316L sample after potentiodynamic testing, we can see that some intergranular corrosion has occurred. Thus, the polypyrrole coating cannot completely prevent corrosion. However, comparing this sample with the uncoated SS316L, Fig. 2c, there is less corrosion evident after polypyrrole coating.

3.7. Potentiostatic tests simulating the PEMFC working conditions

In actual PEMFC working conditions, the anode is at a potential of about −0.1 V versus SCE and the cathode is at a potential of about 0.6 V versus SCE. Under these PEMFC conditions, any corrosion that takes place is not the same as free potential corrosion. In order to study the corrosion behavior of metallic bipolar plates in actual PEMFC working conditions, potentiostatic tests were conducted at −0.1 V versus SCE purged with H_2 to simulate the anode working condition and at 0.6 V versus SCE purged with O_2 to simulate the cathode working conditions. Uncoated SS316L and selected polypyrrole-coated SS316L were chosen for these potentiostatic tests. In the potentiostatic tests, it took less time for the uncoated SS316L to achieve a stable current density than the polypyrrole-coated SS316L: the time for potentiostatic testing was, therefore, 1 h for uncoated SS316L and 2 h for coated SS316L. The test results are shown in Figs. 9 and 10, for the simulated cathode and anode conditions, respectively.

From Fig. 9, which is the simulated cathode working conditions, we can see that the current density of uncoated SS316L stabilizes at about 4×10^{-6} to 5×10^{-6} A cm^{-2} after 500 s, but that it takes more time for polypyrrole-coated SS316L to obtain a stable current density. For the coated samples, the current density gradually decreased to about 1.0×10^{-5} A cm^{-2} after 2 h. It seems surprising that the corrosion current increases after coating with polypyrrole, but this is because the polypyrrole coating is oxidized at 0.6 V versus SCE, which is consistent with other

researcher's findings [9]. This is similar to the results from the potentiodynamic tests (Fig. 7). Also from Fig. 9, we can see the polypyrrole coatings produced using the different methods and processing parameters exhibit almost the same corrosion current densities. The possible reason is that some polypyrrole is oxidized to maintain such a small current density.

Fig. 10 presents the potentiostatic testing results for the simulated anode conditions. For uncoated samples, the current density becomes negative after 50 s. However, for the coated samples, the current density is negative right from the start of the potentiostatic tests and stabilizes at about -1.0×10^{-5} to -2.0×10^{-5} A cm^{-2}. The current density for polypyrrole-coated SS316L becomes negative right away because the corrosion potential is increased after coating with polypyrrole. This negative current density can provide cathodic protection for the metallic bipolar plate material. The negative current arises because of the following reactions:

$$2H^+ + 2e^- \rightarrow H_2, \quad \text{metal electrode} \tag{2}$$

$$2H_2O \rightarrow 4H^+ + O_2 + 4e^-, \quad \text{platinum electrode} \tag{3}$$

A more detailed explanation for the negative current density is given in one of our earlier papers [16]. Although no corrosion occurs for either uncoated or polyprrole-coated SS316L at -0.1 V versus SCE purged with H_2 because the current density is negative, in real PEMFC working conditions, the potential could fluctuate and the metal could be corroded.

4. Conclusions

Polypyrrole films have been electro-polymerized on SS316L using both galvanostatic and cyclic voltammometric methods. Comparing the polypyrrole coatings formed using the two different electrochemical methods, the morphologies are quite different. For galvanostatic coatings, the particle size increases with increasing applied current. For cyclic voltammometric coatings, the particle size increases with increasing cycle number. For a low current and low cycle number coating, the polishing marks can still be seen on the SS316L substrate. The potentiodynamic tests show that the corrosion potential is increased from -0.27 to 0.171 V and the corrosion current density is decreased from 40.01 to 2.38 μA cm^{-2} and polarization resistance is increased from 328 to 3459 Ω cm^2 by coating with polypyrrole. Optical microscopy showed that there is less intergranular corrosion after coating with polypyrrole. However, in the simulated cathode environments of a PEMFC, we did not see a reduction in corrosion current because polypyrrole can be oxidized at 0.6 V. In the simulated anode environments of a PEMFC, the current density immediately becomes negative at -0.1 V. This is because the corrosion potential is increased after the polypyrrole coating. A negative current can provide cathodic protection for the SS316L substrate.

Acknowledgements

The authors would like to thank Mr. John Robinson for his assistance with the SEM examination. The research was financially supported by the Natural Sciences and Engineering Research Council of Canada (NSERC) through a Discovery Grant awarded to Prof. D.O. Northwood.

References

[1] I. Bar-On, R. Kirchan, R. Roth, J. Power Sources 109 (2002) 71–75.
[2] H. Tsuchiya, O. Kobayashi, Int. J. Hydrogen Energy 29 (2004) 985–990.
[3] A. Hermann, T. Chaudhuri, P. Spagnol, Int. J. Hydrogen Energy 30 (2005) 1297–1302.
[4] D. Kumar, R.C. Sharma, Eur. Polym. J. 34 (1998) 1053–1060.
[5] N. Cunningham, D. Guay, J.P. Dodelet, Y. Meng, A.R. Hill, A.S. Hay, J. Electrochem. Soc. 149 (7) (2002) A905–A911.
[6] K. Shah, Y. Zhu, J.O. Iroh, O. Popoola, Surf. Eng. 17 (5) (2001) 405–412.
[7] G.S. Akundy, J.O. Iroh, Polymer 42 (2001) 9665–9669.
[8] S. Joseph, J.C. McClure, R. Chianelli, P. Pich, P.J. Sebastian, Int. J. Hydrogen Energy 30 (2005) 1339–1344.
[9] M.A. Lucio García, M.A. Smit, J. Power Sources 158 (2006) 397–402.
[10] Y. Wang, D.O. Northwood, 14th Asian-Pacific Corrosion Control Conference, Shanghai, China, October 21–24, 2006.
[11] H. Wang, J.A. Turner, J. Power Sources 128 (2004) 193–200.
[12] D.A. Jones, Principles and Prevention of Corrosion, first ed., Macmillan, New York, 1992, p. 147.
[13] L. Ma, S. Warthesen, D.A. Shores, J. New Mater. Electrochem. Syst. 3 (2000) 221–228.
[14] M.P. Brady, K. Weisbrod, I. Paulauskas, R.A. Buchanan, K.L. More, H. Wang, M. Wilson, F. Garzon, L.R. Walker, Scripta Mater. 50 (2004) 1017–1022.
[15] W.F. Smith, Foundations of Materials Science and Engineering, third ed., McGraw-Hill, New York, 2004, p. 702.
[16] Y. Wang, D.O. Northwood, International Symposium on Solar-Hydrogen-Fuel Cells, Cancun, Mexico, August 20–24, 2006.